Table S1: Demographics of donors and input datasets derived from donors

Specimen ID	A-P (cms)	Bi temporal diameter (cms)	Brain weight (gms)	Age (GW)
S1 /FB3	6.2	4.6	50	21
S2/ FB10	6.6	5.1	56.24	21-22
S3/ FB36	2.8	3	7	13-14
S4/ FB63	2.8	2.3	6	13
S5/ FB40	4.4	2.8	8.62	14-15

S2: Summary of available atlases and volumes of fetal brain development

Table A Histology based atlases of human brain development

Features	**Bayer and Altman (2005)**[1]	**Allen Brain Institute human developmental atlas**[2]
Details of dataset	2D print atlas (300dpi)	2D digital (1 um/pixel) available online
Number of brains/age	9 whole brains/ 13.5to 24GW	2 Hemispheres - 17GW(15PCW), 23GW(21PCW) and one brainstem 23GW(21PCW)
Annotated sections	88 annotations across 9 brains	168 annotations across the 3 samples
Maximum number of annotations per brain	20	81
Section thickness	35um	20um
Spacing between sections	Variable and uneven	250-1200um
Embedding	Celloidin	OCT
Staining	Nissl and Myelin for older brains	Nissl/ ISH/ AchE/ Myelin for older brains

Table B MRI based data volumes and atlases of human brain development

Atlas/Vol	**Information**			**Atlas Generation method**				
	Modality	**Age (GW)**	**Resolu -tion**	**Registration**	**Atlas construc -tion**	**Kernel regression**	**N**	**Metho d details**
Habas et al., 2010[3]	T2w	21-24	0.5mm	Elastic deformation based on tissue maps	Group-wise	No	20	1.5 T 1x1x3 mm^3
Serag et al., 2011[4]	T2w	23-37	1.18m m	Affine + Bspline free form deformation	Pairwise	Adaptive Gaussian kernel	80	1.5T 1.25×1. 25×2.5 mm^3
Zhan et al., 2013[5]	Post-mortem T2w	15-22	–	SyN in ANTs	Group-wise	No	34	7T 0.19×0 .19×0. 5mm^3 or 0.23×0 .23×0. 5mm^3
Dittrich et al., 2014[6]	Ventricle only	20 - 30	0.78-0.9mm	Semi-supervised learning	–	Gaussian kernel	32 + 12*	1.5T 0.78-0.9

								mm (x,y) 3-4.4mm slices
Wright et al., 2015[7]	Cortical Surface Atlas	23-37	–	Surface registration based on sulcal alignment		Gaussian kernel	80	1.5T
Gholipour et al., 2017[8]	T2w	21-37	0.8mm	Greedy SyN in ANTs	Group-wise	Fixed-width Gaussian kernel	81	3T or 1.5T 0.9~1.1-2mm slices
Xia et al., 2019[9]	Cortical Surface Atlas	26.5, 27, 28.2, 28.7		Surface registration	–	No	25	1.5T 0.5×0.5×2.5 mm^3
Li et al., 2021[10]	T2w	23-36	0.8mm	Affine + SyN in ANTs	Pairwise + group-wise	No	212	1.5T 0.74×0.74×4 mm^3
Wu et al., 2021[11]	T2w	22-35	0.8mm	SyN in ANTs	Group-wise	Adaptive Gaussian kernel	735	1.5T 4mm slice
Uus et al., 2021[12]	T2w	21-36	0.7mm	MIRTK atlas generation pipeline	–	Gaussian kernel	291	3T 1.1×1.1×2.2 mm^3
Xu et al 2022[13]	T2w	23-38	0.8mm	ANTs Rigid+affine+SyN	Pairwise +group-wise	Adaptive Gaussian kernel	219	3T 1.1×1.1×2 mm^3

*abnormal brains

Abbreviations: GW = gestational age; SyN = symmetric diffeomorphic deformable registration algorithm; ANTs = advanced normalization tools.

References

1. Bayer, S. A. & Altman, J. *The Human Brain During the Second Trimester*. (CRC Press, 2005). doi:10.1201/9780203507483.
2. Ding, S.-L. *et al.* Cellular resolution anatomical and molecular atlases for prenatal human brains. *J Comp Neurol* **530**, 6–503 (2022).
3. Habas, P. A. *et al.* A spatiotemporal atlas of MR intensity, tissue probability and shape of the fetal brain with application to segmentation. *NeuroImage* **53**, 460–470 (2010).

4. Serag, A. *et al.* Construction of a consistent high-definition spatio-temporal atlas of the developing brain using adaptive kernel regression. *NeuroImage* **59**, 2255–2265 (2012). http://brain-development.org/
5. Zhan, J. *et al.* Spatial–temporal atlas of human fetal brain development during the early second trimester. *Neuroimage* **82**, 10.1016/j.neuroimage.2013.05.063 (2013). http://www.loni.ucla.edu/Atlases/
6. Dittrich, E. *et al.* A spatio-temporal latent atlas for semi-supervised learning of fetal brain segmentations and morphological age estimation. *Medical Image Analysis* **18**, 9–21 (2014).
7. Wright, R. *et al.* Construction of a fetal spatio-temporal cortical surface atlas from in utero MRI: Application of spectral surface matching. *NeuroImage* **120**, 467–480 (2015).
8. Gholipour, A. *et al.* A normative spatiotemporal MRI atlas of the fetal brain for automatic segmentation and analysis of early brain growth. *Scientific Reports* **7**, 476 (2017). http://crl.med.harvard.edu/research/fetal_brain_atlas/
9. Xia, J. *et al.* Fetal cortical surface atlas parcellation based on growth patterns. *Human Brain Mapping* **40**, 3881–3899 (2019).
10. Li, H. *et al.* Mapping fetal brain development based on automated segmentation and 4D brain atlasing. *Brain Struct Funct* **226**, 1961–1972 (2021).
11. Wu, J. *et al.* Age-specific structural fetal brain atlases construction and cortical development quantification for chinese population. *NeuroImage* **241**, 118412 (2021). https://github.com/DeepBMI/FBA-Chinese
12. Uus, A. *et al.* Multi-Channel 4D Parametrized Atlas of Macro- and Microstructural Neonatal Brain Development. *Front Neurosci* **15**, 661704 (2021). https://gin.g-node.org/SVRTK
13. Xu, X. *et al.* Spatiotemporal Atlas of the Fetal Brain Depicts Cortical Developmental Gradient. *J. Neurosci.* **42**, 9435–9449 (2022). https://github.com/Thea-Eddie-Amy/CHN-fetal-brain-atlas

S3: Stereology correction factor

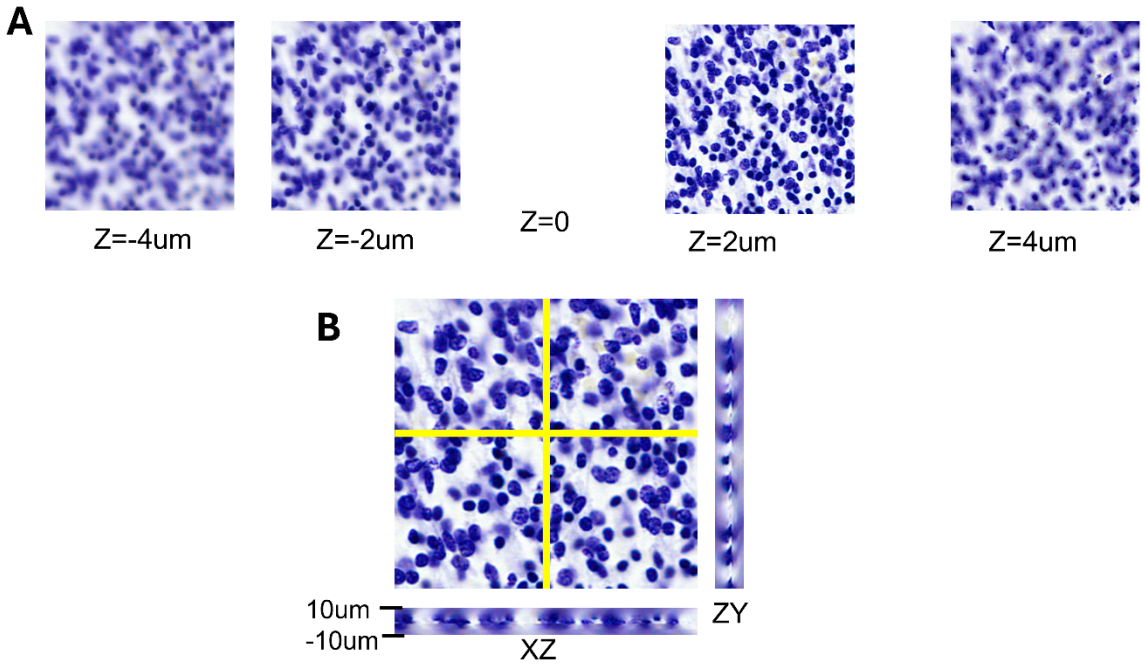

Figure 1 A shows the panel of images obtained as a z-stack (of z-resolution = 1um) of a Thionin-stained section from the 21GW fetal brain. Panel B shows the in-plane focused image (z=0) along with z-cross sections (marked as ZY and XZ) across the x and y planes given by the yellow lines.

We calculated the correction factor and the post-processing effective thickness for computing the cell densities using a z stack of images (1um z-resolution) obtained by our imaging system (Huron LE 120). Figure S xx shows the z stack of images of a thionin-stained section of 20 um thickness. Panel A shows the z stack of images that are focussed between -4um to +4um from an image deemed to be the in-focus plane. Panel B shows the in-plane focussed image and the corresponding z slices in the X and Y axis respectively. This method was performed on several randomly chosen regions with varying cell densities to derive the correction factor.

We calculated the following

1) The thickness of the section (T) was assumed to be 20 um
2) The centres of detected cells within the in-plane focussed sections were marked as mask (A).
3) As one moves through the z-stack of images, any cells that were potentially out of focus were appended to the original detection
4) The correction factor (ϸ or rho) was calculated as a ratio of the total detected cells and the detected cells in the focussed plane.
5) Section densities were calculated as (A x ϸ)/T.

Using this method, we were able to estimate the average correction factor for the whole brain as 1.04. By observing the effective foci of objects within the section, we could estimate the post-processing thickness of sections, which shows a shrinkage following histological processing. In the example shown above, the objects were in focus only in 14 out of 20 sections within the z-stack. The post-processing thickness estimate for the random samples across the tissue sample was between 13-15 um.

S4: Quantifying regional growth in cell counts in the developing human brain: literature review

Despite the large literature on neurogenesis and brain development, very few studies (table 1) have numerically quantified cell counts in the developing human brain, and all previous studies are based on statistical sampling approaches. Previous studies have methodological challenges including non-uniform and sparse statistical sampling, assumptions and/or stereological correction factors, which add to the sample procurement and fixation issues commonly associated with fetal brains.

Earlier, methods such as estimation of DNA weights as a surrogate of cellular growth showed that there is a rapid exponential growth between 10-18 GW followed by a slower phase of expansion after 20GW[1]. H-Thymidine DNA was used as a marker to show that almost all cortical neurogenesis takes place in the first phase of pregnancy[2,3]. More recently, quantification of cellular counts as a function of developmental time was achieved using histology based methods based on random sampling and the extrapolation of cell counts using the optical fractionator approach, in a very limited number of studies[4–8] . Further, regional cell counts have been confined to the developing cortex[7].

We provide the first comprehensive cell counts based on machine-vision based detection and counting of cells in closely spaced histological sections across the whole brain, which do not suffer from the sparse sampling limitations of the previous studies. In addition, we also provide the first regional counts in a comprehensive set of compartments including subcortical structures. A comparison between our counting estimates and literature data (Table 2) shows that where these estimates exist, they are generally consistent with our findings.

Table 1 Human brain development cell counts

Ref	Method	Age /n	Whole brain/ parts	Output relevant to this paper
Histology based cell counts				
Samuelsen et al 2003[7]	Cell counts with histology GIEMSA 40um paraffin sections	13- 42 GW (n=22)	Human fetal telencephalon	Random sampling within sections (100 objects per view) x 10 -12 sections per brain Estimated cell counts= 4.5 billion (13 GW) 15 billion (21 GW)
Larsen et al 2006[5]	Cell counts with histology GIEMSA 40um paraffin sections	New-Born (38-42 GW n=10)	Human fetal telencephalon	Random sampling within sections (100 objects per view) x 10 -12 sections per brain The mean total cell number was 32.6 billion cells (coefficient of error=0.04)
Samuelsen et al, 2007[6]	Cell counts with histology GIEMSA 40um paraffin sections	18-42 weeks GW	Human fetal telencephalic wall	Estimated cell counts = 15.45 Billion cells (21GW) (same samples as previous paper?)
Rabinowicz et al 1996[4]	Cell counts with histology	17 GW to 17	Regions -Precentral gyrus	Estimated cell density = 6000 cells/0.001mm^3 (21 GW) 4000 cells/0.001mm^3 (17 GW)

	Cresyl violet 10-25um Paraffin sections	weeks post birth (n= 9)	-Wernicke's area -Broca's area -Calcarine cortex -Cingulate cortex -Frontal pole	
Other methods (qualitative no cell counts)				
Rakic & Sidman, 1973[2]	H-thymidine DNA	<6 – 16GW	Radiological	Shows neuronal differentiation from progenitors happens only in early gestation
Dobbing and Sands, 1973[1]	pDNA and Cholesterol	10GW to 8 years post birth	pDNA (weight per volume)	Qualitative showing two phases of growth : 1st rapid phase between 10-20 GW and a slower growth from 20GW

Table 2 shows the comparison of total and regional cell counts of the fetal brain available in the literature compared to our current study. The literature data is derived from studies using the optical fractionator methods.

Region	**Rabinowicz et al 1996**[4]	**Samuelsen et al 2000**[8]	**Samuelsen et al 2003**[7]	**Samuelsen et al 2007**[6]	**This paper**
Total	6000 cells/mm^3 (*21GW*) = 7.5 x10^9 (assuming 50 x 50 x 50 mm)		*13GW* 3.01 x 10^9 *20 GW* 12.8 x 10^9 *22GW*= 16.7 x 10^9	*22GW* 16.7 x 10^9	*13GW* 3.7 x 10^9 *21GW* 17.4 x 10^9
MZ/CP	-	*22GW* 5.7 x 10^9	*13GW* 0.96 x 10^9 *20GW* 5.87 x 10^9 *22GW* 7.05 x 10^9	-	*13GW* 0.02x 10^9 (MZ) and 0.73 x 10^9 (CP) *21GW* 0.26 x 10^9 (MZ) and 5.3 x 10^9 (CP)
SP	-		*13GW* 0.66 x 10^9 *20GW* 2.4 x 10^9 *22GW* 1.9 x 10^9	-	*13GW* 0.77 x 10^9 *21GW* 2.6 x 10^9
IZ	-	*22GW* 2.2 x 10^9	*13GW* 0.8 x 10^9 *20 GW* 3.06 x 10^9 *22GW*	-	*13GW* 0.80 x 10^9 *21GW* 3.82 x 10^9

			2.58x 10^9		
VZ/SZ	-	*22GW* 5.1 x 10^9	*13GW* 0.57 x 10^9 *20GW* 1.44 x 10^9 *22GW* 4.58 x 10^9	-	*13GW* 0.25 x 10^9 (SZ) and 0.24 x 10^9 (VZ) *21GW* 0.96 x 10^9 (SZ) and 0.12 x 10^9 (VZ)

References

1. Dobbing, J. & Sands, J. Quantitative growth and development of human brain. *Arch Dis Child* **48**, 757–767 (1973).
2. Sidman, R. L. & Rakic, P. Neuronal migration, with special reference to developing human brain: a review. *Brain Res* **62**, 1–35 (1973).
3. Rakic, P. & Sidman, R. L. Supravital DNA Synthesis in the Developing Human and Mouse Brain. *Journal of Neuropathology & Experimental Neurology* **27**, 240–276 (1968).
4. Rabinowicz, T., de Courten-Myers, G. M., Petetot, J. M.-C., Xi, G. & de los Reyes, E. Human Cortex Development: Estimates of Neuronal Numbers Indicate Major Loss Late During Gestation. *Journal of Neuropathology & Experimental Neurology* **55**, 320–328 (1996).
5. Larsen, C. C. *et al.* Total number of cells in the human newborn telencephalic wall. *Neuroscience* **139**, 999–1003 (2006).
6. Samuelsen, G. B. *et al.* Severe cell reduction in the future brain cortex in human growth–restricted fetuses and infants. *American Journal of Obstetrics and Gynecology* **197**, 56.e1-56.e7 (2007).
7. Samuelsen, G. B. *et al.* The Changing Number of Cells in the Human Fetal Forebrain and its Subdivisions: A Stereological Analysis. *Cerebral Cortex* **13**, 115–122 (2003).
8. Samuelsen, G. B. *et al.* TOTAL CELL NUMBER IN FETAL BRAIN. *Image Analysis and Stereology* **19**, 35–38 (2000).

S5: Evaluation of the detection of mitotic figures in H&E

We evaluated the markings and detections of mitotic figures in the H&E sections by comparing them with adjacent sections stained with immunohistochemistry of the proliferative marker Ki-67. Figure 1 shows two regions from the H&E stained histological section (A) and the adjacent section stained using DAB-based immunohistochemistry of the Ki-67. As shown in the figure, the detection of mitotic figures in the H&E stained sections are limited by the relative contrast of the stain. The Ki-67 antibody stain provided more contrast and more mitotic figures could be detected. Examination of the relative numbers and spacing of the mitotic figures detected in the Ki-67 stained sections, showed a ratio of about two. This implies that the mitotic figures visually detected in the H&E sections may be underestimating the correct number by a factor of two.

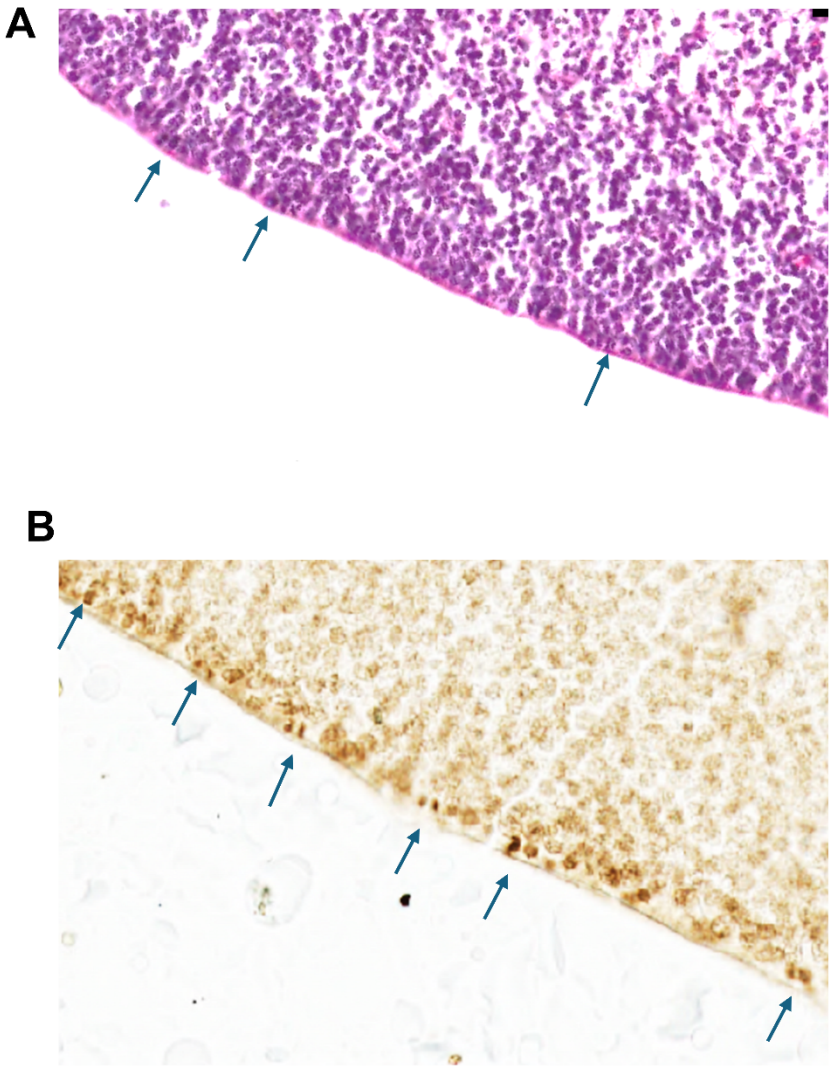

Figure 1 shows detected mitotic figures in the ventricular zone (VZ) of a section stained with H&E (A) and an adjacent section stained for Ki-67, a proliferative marker (B). The arrows show the detected mitotic figures in both staining.

Nomenclature for developing brain compartments

The existing nomenclature for atlas compartments of the developing human brain is complex and includes names and abbreviations of not only the evolving brain parts (brain regions, fiber tracts and ventricles but also the transitive developmental structures, such as the ganglionic eminence and the migratory streams.

Problems associated with atlas nomenclatures and our approach based on coordinate frameworks and a flat list of cytoarch1tectonic regions: Brain atlases have named compartments, with the terminology for mammals being derived from the early work of His[1]. Over time, there has been a proliferation of atlases that differ in compartment boundaries and nomenclatures. Even within a given species, there are multiple atlases with nomenclatures that are not easy to reconcile. In humans, the complexity is higher owing to the larger number of distinct anatomical parcellations. In addition to the challenges that exist for adult atlas nomenclature, development atlases add the extra dimension of time. Adult atlases may be regarded as parcellations of brain space. Developmental atlases conceptually require a parcellation of developmental space-time, considering the formation of new compartments at relevant developmental time points as well as the disappearances of transient structures. Even if a compartment remains trackable throughout development, functional nomenclature appropriate for the adult may not be appropriate for the developing fetus. For these reasons, it is preferable to move towards a common coordinate system-based approach, where a specific location in the brain at a particular age is specified using an appropriate three-dimensional coordinate in a reference brain.

This has been our motivation in focusing on the coordinate framework and reference brain volumes in the current manuscript. Nevertheless, to maintain continuity with the literature we also provide a parcellation and nomenclature for the developmental ages under study in the manuscript. We adopt an approach developed earlier[2] in which we prioritize a parcellation of the brain into non-overlapping compartments, the union of which gives back the entire brain space. The parcels are chosen to have visibly well-defined boundaries based on cytoarchitectonic differences across boundaries at a given age. We do not focus on how to group those parcels into a hierarchy since that is often the origin of the debates between neuroanatomists. Some high-level groupings are obvious and canonical and may be easily layered on top of the lowest level parcels.

Discussion of previous atlases and nomenclatures of the developing human brain: The relevant nomenclature for developing mammalian brains has largely been derived so far from developmental studies in model organisms, mostly rodents and primates. This includes parcellations based on a hierarchical gene nomenclature (The Gene Ontology[3]) with more than 500 directly related terms that are associated with textual definitions, and references and models the development of a neuronal structure to the developmental process (e.g., “telencephalon development is part of forebrain development”;[3]). However, this approach is also limited as it does not fully address the spatial and temporal aspects of the brain development and does not reconcile the problem of different nomenclatures within the same species. Puelles and colleagues[4] have attempted to reconcile the classical nomenclature with gene expression patterns and those derived from embryonic prosomeres[4,5]. The problem of the developing cortical regions was addressed by the Boulder Committee nomenclature[6,7], however, this nomenclature leaves out subcortical regions.

The widely accepted print atlas of human brain development by Bayer and Altmann[8] uses nomenclature derived from adult brain atlases/textbooks supplemented with Bayer and Altmann’s own work on rat brain development[9]. This atlas, however, has conflicting names particularly for the developing cortical zones, referred to as the Stratified transitional fields in their publications. More recently, developmental human brain nomenclature was developed for 15 PCW and 22 PCW brains by the Allen Brain Institute[10], in an attempt to reconcile the ontology used by the Boulder Committee and the adult brain atlases. These authors provide a hierarchically organized nomenclature that include more than 3000 terms for both the fetus and adult human brain. These terms include names for adult brain regions which are based on “function” which are questionable when applied to fetal brains as there is little experimental basis for such functional

designation. Further, several terms are included which are not associated with textual definitions, and not all of the terms are are associated with atlas delineations.

Details of our approach: As previously discussed, our focus has been on establishing a reference coordinate system based on skull landmarks, with the idea that atlas parcellations or annotations may be regarded as superposed layers on top of the underlying coordinate system in the reference brains we present. For atlas annotation purposes we have carried out a histology and cytoarchitecture based parcellation of the entire brains involved, while maintaining correspondence with known brain atlases[7,8,10]. Regarding nomenclature, we therefore focus on a flat list of names of these compartments. Table 1 below highlights the marked regions for the plates of histological samples used in this study namely the 13 GW and 21 GW fetal brains.

The list of names we use in this manuscript to designate nonoverlapping compartments include 119 terms presented in the 2D atlas plates as well as in the regional cell count tables. Each term has a name, abbreviation, a textual definition, and a hexadecimal color code used to mark the associated delineations. The terminology included largely follows the nomenclatures proposed by Bayer and Altman[8], AIBS[10], and by the Boulder Committee[6,7] . We also included terms proposed by Zecevic[11], and by Kostovic & Judas[12]. The nomenclature we utilize includes terms and definitions specific only to the human brain, and it is generally not hierarchically organized, although we utilize some generally agreed groupings (eg "thalamus" or "basal ganglia") to summarize our tables of counts, or to assign residual compartments that are not otherwise specified after individual sub-nuclei have been specified.

Table 1 Named brain compartments for the 13GW and 21GW brains relevant to this manuscript

13GW			**21GW**		
ID	**Brain Region**	**Abbr**	**id**	**Brain region**	**Abbr**
10157	gray matter of forebrain	FGM	10157	gray matter of forebrain	FGM
10349	basal forebrain	BF	10349	basal forebrain	BF
11580	subpial granular zone	SG	11580	subpial granular zone	SG
10508	marginal zone	MZ	10508	marginal zone	MZ
10515	cortical plate	CP	10515	cortical plate	CP
10522	subplate zone	SP	10506	subplate zone	SP
10529	intermediate zone	IZ	10529	intermediate zone	IZ
10536	subventricular zone	SZ	10522	subventricular zone	SZ
10542	ventricular zone	VZ	10542	ventricular zone	VZ
10506	transient structures of forebrain	FTS			
10549	Ganglionic eminence (VZ in basal nuclei)	GE	10549	Ganglionic eminence (VZ in basal nuclei)	GE
10294	hippocampus (hippocampal formation)	HIP	10294	hippocampus (hippocampal formation)	HIP
12170	hippocampal gyrus (formation)	HiF	12170	hippocampal gyrus (formation)	HiF
12162	parahippocampal gyrus	PHG	12162	parahippocampal gyrus	PHG
10361	amygdala	AMY	10361	amygdala	AMY
10312	piriform-entorhinal-amygdaloid area	PEA	10312	piriform-entorhinal-amygdaloid area	PEA
10311	Piriform cortex	Pir	10311	Piriform cortex	Pir

			10317	entorhinal cortex	EC
			10288	insular cortex	ICx
10304	indusium griseum	IG	10304	indusium griseum	IG
10350	septal nuclei	SEP	10350	septal nuclei	SEP
			13076	subcallosal gray zone	ScG
			11634	MZ in insular cortex	iMZ
			11728	CP in insular neocortex	iCP
			11742	CP in entorhinal cortex	CPEC
			13207	SG of the allocortex	alSG
			10513	MZ of the allocortex	alMZ
			10534	IZ of the allocortex	alIZ
			11638	MZ in subicular cortex	MZsub
			11738	CP in subicular cortex	CPsub
			11787	SP in the subicular cortex	SPsub
			11875	IZ in subicular cortex	IZsub
			13280	CP in parasubicular cortex	CPpas
13078	perifornical gray zone	PFG	13078	perifornical gray zone	PFG
10331	basal nuclei	BN	10331	basal nuclei	BN
10334	caudate nucleus	Ca	10334	caudate nucleus	Ca
1.46E +08	Caudate Putamen cell bridges	CaPu	1.46E +08	Caudate Putamen cell bridges	CaPu
			10335	head of the caudate	CaH
10338	Putamen	Pu	10338	Putamen	Pu
10333	Striatum	STR	10333	Striatum	STR
10346	Claustrum	Cla	10346	Claustrum	Cla
10339	nucleus accumbens	NAC	10339	nucleus accumbens	NAC
10342	globus pallidus	GP	10342	globus pallidus	GP
10384	bed nucleus of stria terminalis	BNST	10384	bed nucleus of stria terminalis	BNST
10573	external capsule	extC	10573	external capsule	extC
10581	internal capsule	ic	10581	internal capsule	ic
10559	anterior commissure	ac	10559	anterior commissure	ac
10557	white matter of forebrain	fwm	10557	white matter of forebrain	fwm
10591	stria terminalis	st	10591	stria terminalis	st
10576	fornix	fx	10576	fornix	fx
10561	corpus callosum	cc	10561	corpus callosum	cc
12021	olfactory recess	olr	12021	olfactory recess	olr
10567	posterior commisure	poc	10567	posterior commisure	poc
10644	optic chiasm	oc	10644	optic chiasm	oc
10390	thalamus	THM	10390	thalamus	THM
			10364	central medial nucleus of thalamus	CeM
			10391	dorsal thalamus	DTH

			10397	medial nuclear complex of thalamus	MNC
10464	reticular nucleus of thalamus	R	10464	reticular nucleus of thalamus	R
			10409	Pulvinar of the thalamus	Pul
			10389	subthalamus	SubTH
10465	subthalamic nucleus	STH	10465	subthalamic nucleus	STH
			12101	subcommisural organ	SCO
12247	red nucleus	RN	12247	red nucleus	RN
10451	epithalamus	ETH	10451	epithalamus	ETH
10467	hypothalamus	HTH	10467	hypothalamus	HTH
10556	rostral migratory stream	RMS	10556	rostral migratory stream	RMS
10463	zona incerta	ZI	10463	zona incerta	ZI
13034	substantia innominata	SI	13034	substantia innominata	SI
10462	nucleus of the field of Forel	FF	10462	nucleus of the field of Forel	FF
12181	pretectal region	PTR	12181	pretectal region	PTR
12292	superior colliculus	SC	12292	superior colliculus	SC
12305	inferior colliculus	IC	12305	inferior colliculus	IC
12209	periaqueductal gray	PAG	12209	periaqueductal gray	PAG
10650	white matter of midbrain	mwm	10650	white matter of midbrain	mwm
			10659	cerebellum	CBH
13363	external granular (germinal) zone of lateral hemisphere	CbLTe	13363	external granular (germinal) zone of lateral hemisphere	CbLTe
13364	marginal zone of lateral hemisphere	CbLTm	13364	marginal zone of lateral hemisphere	CbLTm
13366	inner granular cell zone of lateral hemisphere	CbLTi	13366	inner granular cell zone of lateral hemisphere	CbLTi
			13365	Purkinje cell zone of lateral hemisphere	CbLTp
13369	ventricular (germinal) zone of lateral hemisphere	CBlTv	13369	ventricular (germinal) zone of lateral hemisphere	CBlTv
13347	external granular (germinal) zone of the vermis	VeTe	13347	external granular (germinal) zone of the vermis	VeTe
13348	marginal zone of the vermis	VeTm	13348	marginal zone of the vermis	VeTm
13353	ventricular (germinal) zone of the vermis	VeTv	13353	ventricular (germinal) zone of the vermis	VeTv
			13349	Purkinje cell zone of the vermis	VeTp
13350	inner granular cell zone of the vermis	VeTi	13350	inner granular cell zone of the vermis	VeTi
10660	cerebellar deep nuclei	CbDN	10660	cerebellar deep nuclei	CbDN
10664	Rhombic lip	RhL			
10310	optic tract	ot	10310	optic tract	ot

12230	cerebral peduncle (crus cerebri)	cpd	12230	cerebral peduncle (crus cerebri)	cpd
10668	white matter of hindbrain	hwm	10668	white matter of hindbrain	hwm
			10652	surface structures of midbrain	MSS
12462	superior olivary complex	SOC			
10649	gray matter of midbrain	MGM			
12251	substantia nigra	SN	12251	substantia nigra	SN
10661	Pontine nucleus	PN	10661	Pontine nucleus	PN
12406	pons	Pn	12406	pons	Pn
			12346	afferent nuclei of cranial nerves in pons	PnAN
			12405	basilar pons	PnBa
			12416	pontine tegmentum	PnTg
12195	midbrain tegmentum	MTg	12195	midbrain tegmentum	MTg
12645	other nuclei in medullary tegmentum	XMoTg	12645	other nuclei in medullary tegmentum	XMoTg
10662	myelencephalon (medulla oblongata)	Mo	10662	myelencephalon (medulla oblongata)	Mo
			12535	pyramidal part of medulla oblongata	MoPy
12890	spinal cord	SpC	12890	spinal cord	SpC
10460	pineal body	Pin	10460	pineal body	Pin
12270	interpeduncular nucleus	IP	12270	interpeduncular nucleus	IP
12600	inferior olive	IO	12600	inferior olive	IO
			12272	pyramidal decussation	xpy
			10654	gray matter of the hindbrain	HGM
			15544	optic nerve	on
			12331	corticopontine fibers midbrain portion	cpn-m
			1.46E+08	white matter of the spinal cord	swm
			12811	median aperture (foramen of Magendie)	ma4V
			12420	facial nucleus	7N
1.46E+08	transient cell zone in external capsule	Tcete			
12354	superior cerebellar peduncle (brachium conjunctivum)	scp			
12098	cavum pellucidum	Pell			
2.66E+08	corticopontine fibers pontine part	cpn			
12304	diagonal band	dib			
10590	stria medullaris of thalamus	smt			
10568	corona radiata	cor			

12344	interpedunculotegmental tract	iptg			

References

1. His, W. *Die anatomische Nomenclatur: Nomina anatomica*. (Veit, 1895).
2. Mezias, C., Huo, B., Bota, M., Jayakumar, J. & Mitra, P. P. Establishing neuroanatomical correspondences across mouse and marmoset brain structures. *BioRxiv* (2024) **doi:** https://doi.org/10.1101/2024.05.06.592808
3. Hill, D. P., Berardini, T. Z., Howe, D. G. & Van Auken, K. M. Representing ontogeny through ontology: A developmental biologist's guide to the gene ontology. *Molecular Reproduction and Development* **77**, 314–329 (2010).
4. Puelles, L., Harrison, M., Paxinos, G. & Watson, C. A developmental ontology for the mammalian brain based on the prosomeric model. *Trends Neurosci* **36**, 570–578 (2013).
5. Nieuwenhuys, R. & Puelles, L. *Towards a New Neuromorphology*. (Springer International Publishing, Cham, 2016). doi:10.1007/978-3-319-25693-1.
6. Angevine Jr., J. B. *et al.* Embryonic vertebrate central nervous system: Revised terminology. *The Anatomical Record* **166**, 257–261 (1970).
7. Bystron, I., Blakemore, C. & Rakic, P. Development of the human cerebral cortex: Boulder Committee revisited. *Nat Rev Neurosci* **9**, 110–122 (2008).
8. Bayer, S. A. & Altman, J. *The Human Brain During the Second Trimester*. (CRC Press, 2005). doi:10.1201/9780203507483.
9. Altman, J. & Bayer, S. A. Horizontal compartmentation in the germinal matrices and intermediate zone of the embryonic rat cerebral cortex. *Experimental Neurology* **107**, 36–47 (1990).
10. Ding, S.-L. *et al.* Cellular resolution anatomical and molecular atlases for prenatal human brains. *J Comp Neurol* **530**, 6–503 (2022).
11. Zecevic, N. & Verney, C. Development of the catecholamine neurons in human embryos and fetuses, with special emphasis on the innervaton of the cerebral cortex. *Journal of Comparative Neurology* **351**, 509–535 (1995).
12. Kostović, I. & Judaš, M. Embryonic and Fetal Development of the Human Cerebral Cortex. in *Brain Mapping* (ed. Toga, A. W.) 167–175 (Academic Press, Waltham, 2015). doi:10.1016/B978-0-12-397025-1.00193-7.